Multiheterodyne spectroscopy with optical frequency combs generated from a continuous-wave laser

D. A. Long,[1,5] A. J. Fleisher,[1] K. O. Douglass,[2] S. E. Maxwell,[2] K. Bielska,[1,3] J. T. Hodges,[1] and D. F. Plusquellic[4,6]

[1]*Material Measurement Laboratory, National Institute of Standards and Technology, Gaithersburg, Maryland 20899, USA*

[2]*Physical Measurement Laboratory, National Institute of Standards and Technology, Gaithersburg, Maryland 20899, USA*

[3]*Institute of Physics, Faculty of Physics, Astronomy, and Informatics, Nicolaus Copernicus University, Grudziadzka 5, 87-100 Torun, Poland*

[4]*Physical Measurement Laboratory, National Institute of Standards and Technology, Boulder, Colorado 80305, USA*

[5]*e-mail: david.long@nist.gov*

[6]*e-mail: david.plusquellic@nist.gov*

Received February 5, 2014; revised March 6, 2014; accepted March 7, 2014;
posted April 1, 2014 (Doc. ID 206053); published April 24, 2014

Dual-drive Mach–Zehnder modulators were utilized to produce power-leveled optical frequency combs (OFCs) from a continuous-wave laser. The resulting OFCs contained up to 50 unique frequency components and spanned more than 200 GHz. Simple changes to the modulation frequency allowed for agile control of the comb spacing. These OFCs were then utilized for broadband, multiheterodyne measurements of CO_2 using both a multipass cell and an optical cavity. This technique allows for robust measurements of trace gas species and alleviates much of the cost and complexity associated with the use of femtosecond OFCs produced with mode-locked pulsed lasers.

OCIS codes: (300.6310) Spectroscopy, heterodyne; (300.6390) Spectroscopy, molecular; (300.6300) Spectroscopy, Fourier transforms; (230.2090) Electro-optical devices; (120.6200) Spectrometers and spectroscopic instrumentation.
http://dx.doi.org/10.1364/OL.39.002688

Femtosecond optical frequency combs (FOFCs) generated from mode-locked pulsed lasers (MLL) offer an unprecedented combination of wide spectral bandwidth and ultra-narrow frequency component linewidths while serving as absolute frequency references when phase stabilized. These unique properties make FOFCs attractive for applications in laboratory spectroscopy [1–5] and remote sensing [6]. However, due to the wide bandwidth of FOFCs, in many cases each frequency component has only nanowatts of optical power, thus limiting the ultimate sensitivity and potential for use in sub-Doppler spectroscopy. Furthermore, the comb spacing (given by the repetition rate for a pulsed laser) is largely fixed for a given MLL by the physical dimension of the laser cavity. These limitations and others have stimulated interest in the generation of optical frequency combs (OFCs) using continuous-wave (cw) lasers and optical modulators [7–10]. These recent studies have reported the generation of broadband power-leveled OFCs [1,7] largely in response to telecommunication needs such as filterless channelization. In the present study we have performed multiheterodyne measurements of trace gases with OFCs generated using dual-drive Mach–Zehnder electro-optic modulators and a single cw laser.

To optimize bandwidth requirements for detection, multiheterodyne spectroscopy [2–4,11,12] typically utilizes two OFCs with slightly different comb spacings. One of these OFCs probes the gas sample of interest, whereas the other serves as a local oscillator (LO). The two OFCs are then combined on a photodiode for bandwidth compression and detection in the radio frequency (RF) domain. Each optical frequency component of the probe laser exhibits a unique RF beat frequency with the LO in the heterodyne signal, thus allowing for the entire OFC to be simultaneously recorded with a spectrum analyzer. Importantly, this method requires no mechanical motion (unlike Fourier-transform spectroscopy, which uses a moving mirror) and therefore allows for high speed measurements.

A schematic of the present instrument can be found in Fig. 1. The OFCs were generated using dual-drive Mach–Zehnder modulators (MZMs, 20 GHz bandwidth). The use of dual-drive MZMs allows for power leveling of the resultant OFC by attenuation of one of the two drives and control of the phase condition through the use of an external DC bias [7]. These parameters were set prior to a given measurement with no active feedback. Representative optical spectrum analyzer traces of the resulting OFCs with 8 and 18 GHz comb spacings can be found in Fig. 2. Importantly, with appropriate microwave components the comb spacing can be agilely varied from near DC to ≥18 GHz over time scales limited by the tuning speeds of microwave sources (100 μs in our case).

Two OFCs (a probe and LO) whose comb spacings differed by $\delta_{f,\mathrm{mod}} = 24$ kHz were produced from a single external-cavity diode laser using the two MZMs. In addition, a fiber-coupled acousto-optic modulator (AOM) was used to shift one of the OFCs by 100 MHz. This moves the heterodyne signal away from DC, thus reducing the effects of $1/f$ noise, and ensures that each pair of optical frequency components corresponds to a unique RF frequency.

In order to normalize probe-LO heterodyne signal, a reference OFC can be added that does not interact with the gas sample. Driving the probe and reference comb AOMs at slightly different frequencies ($\delta_{f,\mathrm{AOM}} = 12$ kHz) produces two interleaved heterodyne signals (see lower panel of Fig. 3). The indicated frequency spectrum corresponds to the magnitude of the Fourier-transformed time-domain signal. The ratio of the n^{th} pair of frequency components yields the normalized transmission signal at the probe frequency, $f_{n,\mathrm{Probe}}$. This is a complex quantity containing phase and

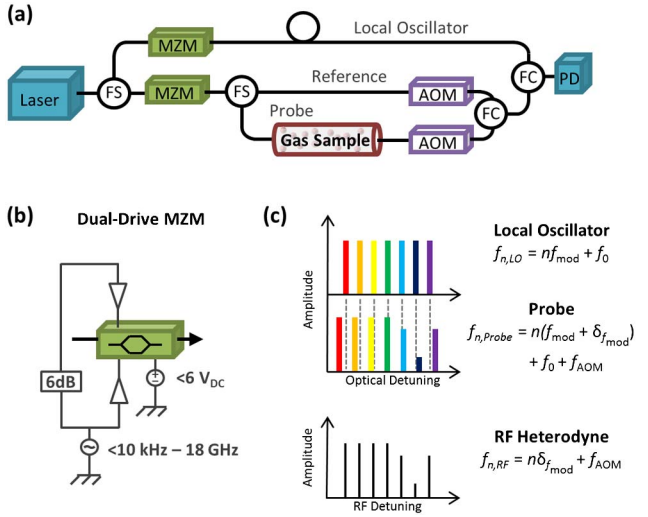

Fig. 1. (a) Schematic of the multiheterodyne spectrometer. FS and FC denote fiber splitters and fiber combiners, respectively. (b) Schematic of the drive signals applied to each dual-drive MZM. An RF signal generated by a fast-switching microwave source is split and amplified into the two drive legs. Microwave powers as high as 2 W were utilized to generate wide OFCs. Attenuation of one of the drives (6 dB) as well as the applied DC bias allowed for power-leveling of the resulting comb. (c) Illustration of the multiheterodyne method. The LO shifts the probe OFC into the RF domain where it can be readily digitized, thus allowing for high-speed multiplexing. Note that f_0 is the optical carrier frequency, n is an integer, f_{AOM} is the frequency of the AOM, f_{mod} is the LO MZM drive frequency, and $\delta_{f,\mathrm{mod}}$ is the frequency difference between the LO and probe MZMs.

amplitude information. The magnitude of this transmission signal is proportional to the field amplitude of the probe laser after passing through the absorbing sample, and therefore equals the square root of the transmission signal normally measured as a ratio of intensities. The phase of the heterodyne signal is also sensitive to the dispersive phase shift of the probe beam, which is caused by propagation through the absorbing medium.

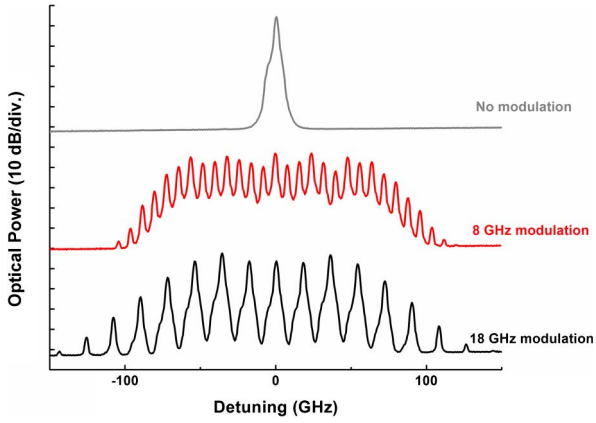

Fig. 2. Optical spectra recorded with an optical spectrum analyzer having a resolution of 4 GHz. The characteristic shape is a product of the spectrum analyzer. Through the use of dual-drive MSMs we have produced power-leveled OFCs with spacings from near DC to 18 GHz. OFCs have been produced with more than 50 individual frequency components.

Transmission measurements were made using two different absorption cells: a fiber-coupled multipass cell and a high-finesse optical cavity. The multipass cell had a total path length of 80 cm (four passes) and was filled with 13 kPa of CO_2. The spectrometer utilizing the fiber-coupled multipass cell has the advantage of being entirely fiber-coupled and therefore ruggedized. Absorption spectra were recorded with a variety of comb spacings and yielded a noise-equivalent absorption coefficient (NEA) of 2×10^{-5} cm^{-1} Hz$^{-1/2}$ per square root of the number of spectral elements [calculated as $\alpha_{\mathrm{min}}(T/M)^{1/2}$, where α_{min}, T, and M are the minimum detectable absorption, acquisition time, and number of spectral elements, respectively]. In order to improve our detection sensitivity, additional measurements were made using an optical cavity (empty-cavity finesse of 20,000).

To ensure constant and efficient coupling of the OFC into the optical cavity, the carrier frequency of the probe laser was Pound–Drever–Hall locked [13] to the optical cavity with a locking bandwidth of 1 MHz, leading to a linewidth of 130 Hz relative to the optical cavity [14]. The spacing of the probe OFC was set to a multiple of the cavity's free spectral range (203.076 MHz), ensuring simultaneous cavity transmission of all probe OFC frequency components. Representative measured phase and amplitude spectra (symbols) and corresponding least-squares fits (lines) can be found in Fig. 3.

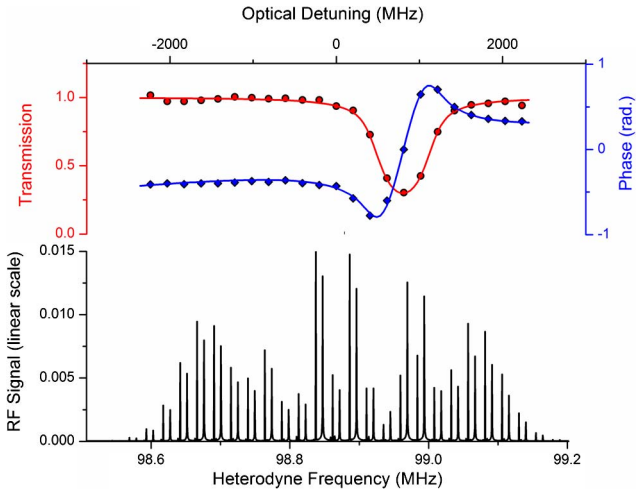

Fig. 3. (Lower panel) Amplitude of the observed multiheterodyne signal resulting from the interference of the OFCs. This signal is the average of 10,000 individual measurements, which were recorded on a 14-bit spectrum analyzer with a bandwidth of 1 kHz in a total time of 30 s. The total optical power on the photodiode was 11.6 μW. Note that due to the common-mode nature of this multiheterodyne signal, the widths of the individual features are resolution limited even at a bandwidth of 1 Hz. The ratio of each probe frequency component and its corresponding reference frequency component yields the local, complex, normalized transmission signal. (Upper panel) Baseline-corrected transmission amplitude (red circles) and phase (blue diamonds) spectra. The two solid lines correspond to a simultaneous fit to the measured amplitude and phase spectra, treating the gas pressure, carrier detuning from line center, and baseline amplitude and phase as adjustable parameters. The absorption feature is the (30013)←(00001) $R16e$ CO_2 transition recorded at a pressure of 14 Pa.

We modeled the complex signal by treating the cavity transmission function as a sum of Lorentzian resonances centered about each cavity mode, with respective mode widths given by the ratio of the cavity mode spacing to the local cavity finesse. Mode pulling effects, which were caused by absorption-induced dispersion of the cavity modes and that lead to frequency detuning of each comb tooth about its local cavity resonance, were calculated in terms of the imaginary part of the absorption line profile [5,15]. This model gave the absorption-induced phase shift of the complex heterodyne signal as the arctangent of the ratio of the frequency detuning to the cavity mode half-width. The increased path length of the optical cavity substantially lowered the detection limit. Specifically, analysis of the signal-to-noise ratio of the fitted spectra in Fig. 3 gives an NEA of 3×10^{-10} $\mathrm{cm^{-1}\,Hz^{-1/2}}$ per square root of the number of spectral elements. This NEA is a few orders of magnitude above the quantum noise limit (1×10^{-12} $\mathrm{cm^{-1}\,Hz^{-1/2}}$ per square root of the number of spectral elements) [5], with our measurement being limited by detector noise.

While the electro-optic OFCs generated here offer far less spectral coverage than traditional FOFCs produced with MLLs, they have considerable advantages for targeted studies of selected trace gases. They allow for low-cost ruggedized operation, and remove much of the instrumental complexity associated with constructing a pair of FOFCs. In addition, producing far fewer spectral components enables considerably higher optical power per spectral element, and thus a correspondingly lower ultimate (shot-noise) detection limit. We also note that with an electro-optic OFC, the comb spacing is electronically controlled and can be varied over a wide frequency range, whereas the spacing of an FOFC is largely fixed by the laser construction. Finally, when utilized in a multiheterodyne measurement, generating OFCs from a single cw laser removes the need for complicated locking.

In a multiheterodyne measurement, resolving each individual frequency component requires a very narrow relative linewidth between probe and LO OFCs [2]. If MLLs are utilized to generate the two FOFCs, this condition requires tight phase locking of the two OFCs, a challenging task that limits the generality and robustness of the resulting instrument. In our present instrument, the OFCs are generated from a single diode laser, leading to a common-mode heterodyne signal. As a result we can readily produce heterodyne signals with signal-to-noise ratios of 75 dB for 1 s of averaging (corresponding to an NEA of 4×10^{-11} $\mathrm{cm^{-1}\,Hz^{-1/2}}$ per square root of the number of spectral elements). This quality greatly reduces the instrumental complexity and should allow for routine field and industrial measurements in which laser amplitude and phase fluctuations and mechanical vibrations do not contribute to the observed heterodyne signal.

The described multiheterodyne instrument leverages the recent development of low-drive-voltage electro-optic modulators to enable high-speed, fully multiplexed absorption measurements with high detection sensitivity. This technique does not rely on mechanical motion, thus allowing measurements to be made over timescales as short as a few microseconds (μs). We believe that this instrument is well-suited for measurements of transient species in the laboratory as well as routine and robust trace gas monitoring.

Support was provided by an NIST Innovation in Measurement Science award and the NIST Greenhouse Gas Measurements and Climate Research Program. K. B. was partially supported by the Foundation for Polish Science TEAM Project co-financed by the EU European Regional Development Fund.

References

1. M. J. Thorpe, K. D. Moll, R. J. Jones, B. Safdi, and J. Ye, Science **311**, 1595 (2006).
2. I. Coddington, W. C. Swann, and N. R. Newbury, Phys. Rev. Lett. **100**, 013902 (2008).
3. B. Bernhardt, A. Ozawa, P. Jacquet, M. Jacquey, Y. Kobayashi, T. Udem, R. Holzwarth, G. Guelachvili, T. W. Hänsch, and N. Picqué, Nat. Photonics **4**, 55 (2009).
4. F. Keilmann, C. Gohle, and R. Holzwarth, Opt. Lett. **29**, 1542 (2004).
5. A. Foltynowicz, T. Ban, P. Maslowski, F. Adler, and J. Ye, Phys. Rev. Lett. **107**, 233002 (2011).
6. E. Baumann, F. R. Giorgetta, I. Coddington, L. C. Sinclair, K. Knabe, W. C. Swann, and N. R. Newbury, Opt. Lett. **38**, 2026 (2013).
7. T. Sakamoto, T. Kawanishi, and M. Izutsu, Electron. Lett. **43**, 1039 (2007).
8. M. Kourogi, T. Enami, and M. Ohtsu, IEEE Photon. Technol. Lett. **6**, 214 (1994).
9. V. Ataie, B. P. P. Kuo, E. Myslivets, and S. Radic, *Optical Fiber Communication Conference/National Fiber Optic Engineers Conference 2013*, OSA Technical Digest (online) (Optical Society of America, 2013), PDP5C.1.
10. L. P. Yatsenko, B. W. Shore, and K. Bergmann, Opt. Commun. **282**, 2212 (2009).
11. S. Schiller, Opt. Lett. **27**, 766 (2002).
12. D. W. Chandler and K. E. Strecker, J. Chem. Phys. **136**, 154201 (2012).
13. R. W. P. Drever, J. L. Hall, F. V. Kowalski, J. Hough, G. M. Ford, A. J. Munley, and H. Ward, Appl. Phys. B **31**, 97 (1983).
14. D. A. Long, G.-W. Truong, R. D. Van Zee, D. F. Plusquellic, and J. T. Hodges, Appl. Phys. B **114**, 489 (2014)..
15. K. K. Lehmann, *Cavity-Ringdown Spectroscopy* (American Chemical Society, 1999), pp. 106–124.